Canad. J. Math. Vol. **57** (4), 2005 pp. 844–870

Petrie Schemes

Gordon Williams

Abstract. Petrie polygons, especially as they arise in the study of regular polytopes and Coxeter groups, have been studied by geometers and group theorists since the early part of the twentieth century. An open question is the determination of which polyhedra possess Petrie polygons that are simple closed curves. The current work explores combinatorial structures in abstract polytopes, called Petrie schemes, that generalize the notion of a Petrie polygon. It is established that all of the regular convex polytopes and honeycombs in Euclidean spaces, as well as all of the Grünbaum–Dress polyhedra, possess Petrie schemes that are not self-intersecting and thus have Petrie polygons that are simple closed curves. Partial results are obtained for several other classes of less symmetric polytopes.

1 Introduction

Historically, polyhedra have been conceived of either as closed surfaces (usually topological spheres) made up of planar polygons joined edge to edge or as solids enclosed by such a surface. In recent times, mathematicians have considered polyhedra to be convex polytopes, simplicial spheres, or combinatorial structures such as abstract polytopes or incidence complexes. A *Petrie polygon* of a polyhedron is a sequence of edges of the polyhedron where any two consecutive elements of the sequence have a vertex and face in common, but no three consecutive edges share a common face. For the regular polyhedra, the Petrie polygons form the equatorial skew polygons. Petrie polygons may be defined analogously for polytopes as well. Petrie polygons have been very useful in the study of polyhedra and polytopes, especially regular polytopes. Our central question is this: which polyhedra and polytopes possess Petrie polygons that are simple closed curves? The current work will provide a partial answer. When a Petrie polygon forms a simple closed curve, we say that it is *acoptic*, and when a Petrie polygon fails to be acoptic we will say that it is *self-intersecting*.

As an illustration, consider the Schlegel diagram given in Figure 1. Petrie polygons have been marked using bold lines; the Petrie polygon in (b) is self-intersecting and the Petrie polygon in (c) is acoptic.

Normally, (*e.g.,* [15,28]) convex polytopes appear in one of two presentations. We define a $\mathcal{V}$*-polytope* as the convex hull of a finite set of points in $\mathbb{R}^d$, and an $\mathcal{H}$*-polytope* as the bounded intersection of finitely many closed half-spaces in $\mathbb{R}^d$.

Two polytopes are said to belong to the same *combinatorial type* if their face lattices (*i.e.,* the posets of their faces, ordered under inclusion) are isomorphic. At this

Received by the editors May 14, 2003; revised March 24, 2004.

This paper summarizes the author's doctoral dissertation *Petrie Schemes* completed in 2002 at the University of Washington. The author wishes to thank Branko Grünbaum for his encouragement and support during the development of this research. The author also wishes to thank the anonymous reviewers who made many valuable comments.

AMS subject classification: Primary: 52B15; secondary: 52B05.

Keywords: Petrie polygon, polyhedron, polytope, abstract polytope, incidence complex, regular polytope, Coxeter group.

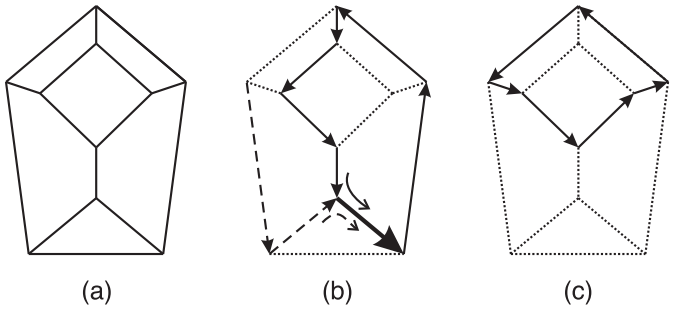

Figure 1: A Schlegel diagram for a polyhedron with a self-intersecting Petrie polygon is given in (a). Part of the self-intersecting Petrie polygon is illustrated in (b), starting with the dashed edges and stopping at the bold edge, which is the first retraced edge. It also possesses an acoptic Petrie polygon shown in (c). This polygon is part of an acoptic Petrie scheme.

time, there is no known computationally feasible technique for determining in general if a given poset corresponds to the face lattice of some convex polytope (for more details see [15, Ch. 5], or [6]). A good example of this is the 3-sphere of McMullen (introduced in his Ph.D. thesis): combinatorially it is highly symmetric, but it is still not known if it is realizable as the boundary of a convex polytope, see [5, 20].

Frequently, polyhedra are defined as closed surfaces in 3-dimensional Euclidean space composed of planar polygons meeting exactly two at an edge, often with the additional requirement that they be *acoptic*, *i.e.,* non-self intersecting. Nothing in such a definition requires that the region bounded by a polyhedron be convex. Thus, there is a natural description available for what constitutes a non-convex polyhedron. Translating this notion to higher dimensional objects, however, presents difficulties which were not present in the convex case. One natural way to extend the notion of non-convex polyhedra to higher dimensions is to consider *simplicial d-spheres*. Unfortunately, there are inconsistencies in the literature about the definition of this term. We will follow Alexander [1]: a simplicial d-sphere is a simplicial subdivision $\mathcal{S}$ of a topological d-sphere such that some refinement of $\mathcal{S}$ is isomorphic to a refinement of the natural simplicial subdivision of the boundary of a $(d+1)$-simplex. This definition is equivalent to another definition for a simplicial d-sphere which is frequently seen in the literature, *e.g.,* [2], in which the the combinatorial simplicial d-sphere is defined inductively as a simplicial complex which is homeomorphic to a d-sphere and in which the link of each vertex in the manifold is a simplicial $(d-1)$-sphere.

Another approach to developing a combinatorial abstraction of polytopes has begun to receive wider attention in recent years. In his seminal paper with Ludwig Danzer, Egon Schulte developed the notion of an *incidence complex* [14], and in subsequent work, principally with P. McMullen [21–25] refined this purely combinatorial structure into what is now commonly referred to as an *abstract polytope*. An abstract polytope is a class of graded posets which generalize certain properties of the face lattice of a convex polytope. Elements of these posets are referred to as *faces*, and

https://doi.org/10.4153/CJM-2005-033-6 Published online by Cambridge University Press

a face F is said to be *contained* in a face G if $F < G$ in the poset. A face at rank i is an *i-face*. A face F is *incident* to a face G if either $F < G$ or $G < F$. A *proper face* is any face which is not a maximal or minimal face of the poset. A *flag* is any maximal chain in the poset, and the *length* of a chain C is $|C| - 1$. Throughout this paper, a flag will be represented by the list of proper faces which determine the flag, omitting the maximal and minimal faces. Following [24] we will require that the poset P also possess the following four properties:

P1 P contains a least face and a greatest face, denoted F_{-1} and F_n respectively.
P2 Every flag of P has the same length, here denoted $n + 1$.
P3 P is strongly connected.
P4 For each $i = 0, 1, \ldots, n-1$, if F and G are incident faces of P, and the ranks of F and G are $i - 1$ and $i + 1$ respectively, then there exist precisely two i-faces H of P such that $F < H < G$.

Note that an abstract polytope is *connected* if either $n \leq 1$ or $n \geq 2$ and for any two proper faces F and G of P there exists a finite sequence of incident proper faces $J_0, J_1, \ldots, J_n$ such that $F = J_0$ and $G = J_n$. A polytope is strongly connected if every section of the polytope is connected, where a *section* corresponding to the faces H and K is the set $H/K := \{F \in P \mid H < F < K\}$. Some texts are more concerned with the notion of *flag connectivity*. Two flags are *adjacent* if they differ by only a single face. A poset is *flag-connected* if for each pair of flags there exists a sequence of adjacent flags connecting them, and a poset is *strongly flag-connected* if this property holds for every section of the poset. It has been shown [24] that for any poset with properties P1 and P2, being strongly connected is equivalent to being strongly flag-connected.

1.1 Outline of Topics

Section 2 will discuss the history and structure of Petrie polygons, and will develop a related structure, called a Petrie scheme. In addition, we will discuss the notion of *Petrial* abstract polytopes, which are polytopes that possess Petrie schemes with the minimal amount of self-intersections.

In Section 3 we will demonstrate that a broad range of geometrically regular polyhedra and polytopes are Petrial.

Finally, in Section 4 we will discuss some other classes of polytopes which are known to be Petrial, and what is known about certain classes of simplicial spheres. We will conclude with some conjectures about other classes of polytopes which the author believes are Petrial.

2 Petrie Polygons and Petrie Schemes

2.1 History

In H. S. M. Coxeter's classic text *Regular Polyopes* [10], the notion of a Petrie polygon was used extensively in the analysis of regular polytopes, especially in the estimation of the sizes of their symmetry groups. Later works, such as those of B. Grünbaum [16], P. McMullen and E. Schulte [24], and S. Wilson [27], used Petrie polygons of regular complexes to derive new complexes which are also regular; these structures

https://doi.org/10.4153/CJM-2005-033-6 Published online by Cambridge University Press

frequently are referred to as *regular maps*.

Some work has also been done to generalize the notion of Petrie polygons to higher dimensions, principally by Coxeter [10], but also by Schulte and McMullen [24] in the context of regular abstract polytopes. In the present work, we present a new generalization of the notion of a Petrie polygon, called a Petrie scheme. In all of the studied examples, the Petrie polygon turns out to be a restriction of the Petrie scheme to a single rank. It is not known whether or not this always works, in the sense that it is conceivable that there exists an abstract polytope having a Petrie scheme that, when restricted to a single rank, might result in retracing a single Petrie polygon several times.

2.2 Basic Concepts and Definitions

A Petrie polygon is a purely combinatorial structure, so we will begin by defining our more general notions in terms of the purely combinatorial setting of abstract polytopes.

A *flag* of an abstract polytope is any maximal chain in the polytope; in geometric polytopes, this is a collection of incident faces $\{f_0, f_1, \ldots, f_d\}$, where each f_i is an i-face and $f_i \subset f_{i+1}$ for each i, so that there is precisely one face from each rank in the collection. Given a flag F, we will occasionally denote the element at rank k in the flag as F_k.

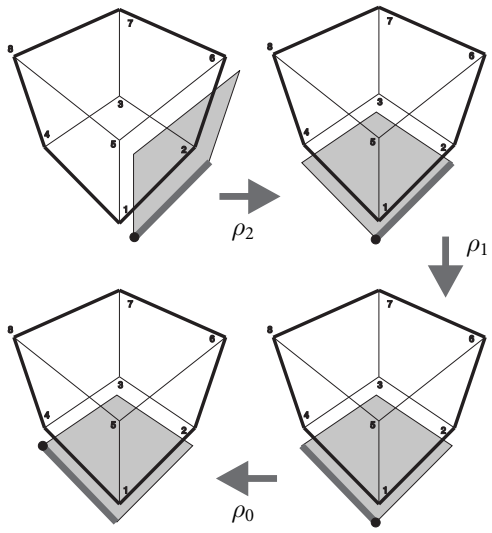

Figure 2: An illustration of how three exchange maps, taken in sequence, form a Petrie map.

An *exchange map* ρ_i is a map on the flags of the (abstract or geometric) polytope sending each flag to the unique flag which differs from it only by the element

https://doi.org/10.4153/CJM-2005-033-6 Published online by Cambridge University Press

at rank i. These exchange maps should not be confused with the reflections in geometrically regular polytopes that have the same action on an individual flag, as they act differently on the other flags of the polytope and are not sufficiently general for use with polytopes that are not regular. A *Petrie map* σ of a polytope P of rank d is any composition of the exchange maps, $\{\rho_0, \rho_1, \ldots, \rho_{d-1}\}$, on the flags of P in which each of these maps appears exactly once (see Figure 2). For example, the map $\sigma = \rho_{d-1}\rho_{d-2}\ldots\rho_2\rho_1\rho_0$ is a Petrie map. Thus, for a polyhedron, there are three exchange maps ρ_0, ρ_1 and ρ_2, and four distinct Petrie maps, $\rho_2\rho_1\rho_0,\ \rho_2\rho_0\rho_1 \equiv \rho_0\rho_2\rho_1,\ \rho_1\rho_2\rho_0 \equiv \rho_1\rho_0\rho_2$, and $\rho_0\rho_1\rho_2$.

In the language of Coxeter groups (see Section 3.1.1), a string Coxeter group W with a string diagram with d nodes and $d-1$ branches marked ∞ admits a permutation representation on the set of flags of any polytope, called the *flag action* of W on the polytope. The exchange maps are the permutations corresponding to the standard (or privileged) generators of W, and the Petrie maps correspond to the Coxeter elements in W. For a description of the flag action in the context of abstract polytopes, see [18].

Definition 2.1 A *Petrie sequence* of an abstract polytope is an infinite sequence of flags which may be written in the form $(\ldots, \sigma^{-1}F, F, \sigma F, \sigma^2 F, \ldots)$, where σ is a fixed Petrie map and F is a fixed flag of the polytope.

Definition 2.2 A *Petrie scheme* is the shortest possible presentation of a Petrie sequence. If a Petrie sequence of an abstract polytope contains repeating cycles of elements, then the Petrie scheme is the shortest possible cycle presentation of that sequence. Otherwise, the Petrie scheme is the Petrie sequence. The *length* of the Petrie scheme is the number of flags in its presentation.

Note that any Petrie sequence in which a flag F appears twice must have a cycle presentation. If k is the smallest integer such that $\sigma^k F = F$, then up to cyclic permutation, the Petrie scheme is $\left(F, \sigma F, \ldots, \sigma^{k-1}F\right)$.

A Petrie scheme in a polyhedron or a convex polytope corresponds to a Petrie scheme of the associated abstract polytope in the natural way. A portion of a Petrie scheme of the cube is illustrated in Figure 3. Using the indicated labeling of the vertices, the illustrated scheme was generated using $\sigma = \rho_2\rho_1\rho_0$ and is given by

$$\Big(\big\{ \{1\}, \{1,2\}, \{1,2,6,5\} \big\}, \big\{ \{2\}, \{2,6\}, \{2,6,7,3\} \big\}, \\ \big\{ \{6\}, \{6,7\}, \{6,7,8,5\} \big\}, \big\{ \{7\}, \{7,8\}, \{7,8,4,3\} \big\}, \\ \big\{ \{8\}, \{8,4\}, \{8,4,1,5\} \big\}, \big\{ \{4\}, \{4,1\}, \{4,1,2,3\} \big\} \Big).$$

We will refer to the sequence of faces obtained by selecting out only those elements of a given rank i in a Petrie scheme as the *rank i elements* of the Petrie scheme. It is easy to demonstrate that the rank 1 elements of a Petrie scheme correspond to the classical notion of a Petrie polygon of a convex polytope.

https://doi.org/10.4153/CJM-2005-033-6 Published online by Cambridge University Press

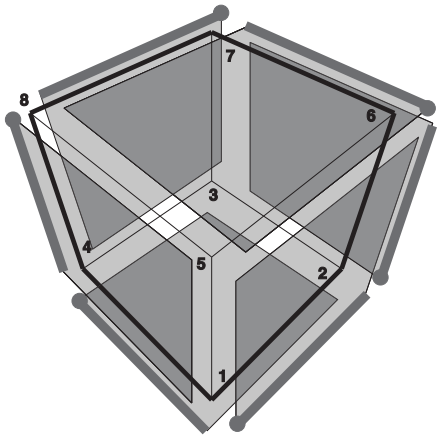

Figure 3: Six flags of a Petrie scheme of the cube illustrated in an exploded view. The Petrie polygon associated with this scheme is indicated by bold black lines.

Definition 2.3 A Petrie scheme is *acoptic* if each proper face appears at most once in the Petrie scheme. An abstract polytope is *Petrial* if all of its Petrie schemes are acoptic.

The term "Petrial" has been used in other contexts, *e.g.,* [24], for the Petrie-dual of a polyhedron. It is important to note that most Petrie schemes (or even Petrie polygons) are not acoptic. The Schlegel diagram of a convex polyhedron which has a Petrie polygon that self-intersects several times before forming a repeating cycle is given in Figure 1. Hence, the polyhedron is not Petrial. On the other hand, it is shown in Section 3.1 that all of the regular convex polytopes possess acoptic Petrie schemes. This leads to the following question: which polytopes (abstract or geometric) have acoptic Petrie schemes? More generally, one may be concerned with classifying those abstract polytopes which are *nearly* Petrial; *i.e.,* which abstract polytopes of rank n possess Petrie schemes which are acoptic for some subset S of the ranks?

Definition 2.4 A Petrie scheme of a polytope P is *S-acoptic*, where S is a subset of the ranks of P, if the rank i elements are distinct for each $i \in S$. We say the polytope is *S-Petrial* if all of its Petrie schemes are S-acoptic.

A polytope that has Petrie schemes which are acoptic on the rank set $S = \{0, 1\}$ possesses Petrie polygons which are simple cycles.

To analyze the Petrie schemes of a polytope, it suffices to look at the schemes generated by a single choice of Petrie map:

Theorem 2.5 *Any two Petrie maps of an abstract polytope are conjugate.*

Proof Central to this argument is a consequence of property P4 of abstract polytopes that if $|j - k| \geq 2$ then $\rho_j \rho_k = \rho_k \rho_j$. The proof of the theorem follows almost

https://doi.org/10.4153/CJM-2005-033-6 Published online by Cambridge University Press

exactly the corresponding argument given in [19, p. 75] for why all Coxeter elements are conjugate in a Coxeter group, although the argument presented there is being applied in the somewhat narrower context of finite reflection groups. ■

3 Petrie Schemes of Regular Polyhedra and Polytopes

3.1 The Regular Convex Polytopes and Their Petrie Schemes

Most of the key facts necessary to demonstrate that all of the regular convex polytopes are Petrial are covered in Humphreys' book *Reflection Groups and Coxeter Groups* [19]. First, some terminology.

Each regular polytope (or polyhedron) may be classified by its combinatorial type. The *Schläfli symbol* is a way of recording the combinatorial type by a sequence of symbols $\{a_1, a_2, \ldots, a_{d-1}\}$, where the first $d-2$ symbols $\{a_1, a_2, \ldots, a_{d-2}\}$ refer to the structure of the faces and the last $d-2$ symbols $\{a_2, \ldots, a_{d-1}\}$ refer to the structures of the links of the vertices. In the simplest case, $\{k\}$ refers to a planar, regular k-gon, and is used to define the longer symbols inductively. For more on Schläfli symbols, see [10, 16]. Grünbaum's article [16] introduces the notation used in Section 3.3 to describe more complicated embeddings of polygons necessary for the construction of certain types of polyhedra.

3.1.1 Coxeter Groups

For consistency of notation and clarity, we include here a brief summary of the structure of a Coxeter group. A Coxeter group is any group possessing a presentation with the conditions that:

(1) it possesses a finite set of generators $\{s_0, s_1, \ldots, s_{n-1}\}$, called the *privileged generators*;
(2) each generator is an element of order 2;
(3) for each pair (i, j) there is an integer $m_{i,j}$ such that $(s_i s_j)^{m_{i,j}} = (s_j s_i)^{m_{i,j}} = e$, where e is the identity element of the group;
(4) $m_{i,j} > 1$ if $i \neq j$.

A Coxeter group acting on $\mathbb{R}^n$ as a reflection group is a *spherical* Coxeter group if it has fixed points and an *affine* Coxeter group if it has no fixed points. A *string* Coxeter group has the added condition $m_{i,j} = 2$ whenever $0 \leq i < j - 1 \leq n - 2$. A string Coxeter group is *irreducible* if $m_{i,j} > 2$ when $|i - j| = 1$. Given a finite spherical Coxeter group W and the set of generating maps $s_0, s_1, s_2, \ldots, s_{n-1}$, a *Coxeter element* ω is any product of those generators in which each generator appears exactly once.

3.1.2 Coxeter Groups and Regular Convex Polytopes

It is known that irreducible spherical Coxeter groups with a string diagram are the symmetry groups of the regular convex polytopes, and that to each choice of base flag F for a regular convex polytope P there is a corresponding set of privileged generators of the Coxeter group, called the *distinguished generators* of P for the flag F. The behavior of the exchange maps of the flags of P restricted to F is the same as that

https://doi.org/10.4153/CJM-2005-033-6 Published online by Cambridge University Press

which arises from the action of the distinguished generators of the symmetry group of P. Thus, there is a correspondence between these two kinds of maps. Because of the correspondence (but not identification) between the classical notion of the generating reflections of a Coxeter group with the exchange maps acting on the base flag corresponding to the privileged generators of the Coxeter group, we will obtain the same sequence of flags iterating under either set of generators when we start with the base flag. On the other hand, it is worth emphasizing that the exchange maps are not (in fact) symmetries, and they behave differently than the privileged generators off the base flag.

In the context of regular convex polytopes, a choice of a set of elements s_i and Coxeter element ω corresponds to a choice of base flag and the generating reflection maps associated with that base flag, and ω acts on that base flag with exactly the same effect as one of the Petrie maps. Thus, for a regular convex polytope to fail to be Petrial, it suffices to show the existence of a choice of base flag F and Coxeter element ω so that for some n, $\omega^n F \cap F \neq \varnothing$ and $\omega^n F \neq F$. In the language of Coxeter groups, this is the same as saying that some power of ω is non-trivial and lies in a (standard) parabolic subgroup of W, where a *parabolic subgroup* of a Coxeter group is any group generated by a proper subset of the privileged generators of the Coxeter group. It is a consequence of some basic facts about Coxeter elements that this cannot happen. Much of the description below benefits from correspondence and conversations with J. Humphreys, E. Babson and W. McGovern.

To understand that no power of ω can lie in a parabolic subgroup of W if W is an irreducible Coxter group, one needs to consider several facts. The *length* of an element of a Coxeter group is the length of the shortest way of expressing it in terms of the privileged generators of the group. It is well known that the length functions on the Coxeter group and on any parabolic subgroup agree for elements in the subgroup, and that if the order h of the Coxeter element is even, then $\omega^{h/2}$ is the longest element in the Coxeter group [19, Ex. 2, p. 82] and its reduced expression must contain each of the generating reflections. In fact, the longest element has a natural expression in terms of two elements y and z which are themselves products of subsets of the generators, where the subsets of generators used in each product commute pairwise. This also proves that lower powers of ω do not lie in parabolic subgroups either, since if any had been reducible there would be a shorter expression for $\omega^{h/2}$. The higher powers of ω less than h have reduced expressions with the elements y and z appearing in reverse order, and so all of the generating symmetries appear as well. A similar argument may be performed in the case when h is odd, using a slightly modified argument (see [7, §6, Ex. 2, p. 151]).

The proof of these facts about a Coxeter element ω involves careful scrutiny of a plane P that is stabilized by the action of ω. The elements y and z are generating reflections of the dihedral subgroup of the Coxeter group which stabilize P, and ω acts as a rotation on P. The representation of $\omega^{h/2}$ in terms of the generators y and z is a consequence of the geometric fact that the map taking one fundamental domain to another is determined by the reflecting planes (the boundaries of the domains) crossed by a path connecting the two domains, and that the reflection lines in P are the intersections of the hyperplanes fixed by y and z with the plane P.

We may thus conclude the following results.

Theorem 3.1 *Let h be the order of a Coxeter element ω in an irreducible, spherical Coxeter group. Then for all $i < h$, ω^i does not lie in a parabolic subgroup.*

Corollary 3.2 *The regular convex polytopes are Petrial.*

In a regular convex polytope the plane in the discussion above bisects each of the edges in a Petrie polygon of the polytope. In fact, to each Petrie polygon (and scheme) of a regular convex polytope there is associated a corresponding Coxeter element and stabilized plane.

Unfortunately, this proof method does not seem to lend itself to an immediate result about the star polytopes described in [10]. It is reasonable, however, to suggest the following.

Conjecture 3.3 *The regular star polytopes are Petrial.*

3.2 The Regular Honeycombs Are Petrial

Throughout this section we are concerned with the regular honeycombs of Euclidean space. For the proof below, we will use the geometric symmetries that produce the same sequence of flags, when acting on our chosen base flag, as would be obtained by applying the exchange maps to the chosen base flag. Given that the objects under consideration are geometrically regular, this is sufficient to prove the desired result.

The main objective of this section is the proof of the following theorem.

Theorem 3.4 *Every regular honeycomb is Petrial.*

3.2.1 The Regular Honeycombs

Following [10], the six types of regular honeycomb of $\mathbb{R}^n$ are given in Table 1. Note that combinatorially, the apeirogon and the cubic honeycomb of $\mathbb{R}^1$ are the same, but their geometric presentations and Schläfli symbols differ, so they are listed seperately.

Table 1: The regular honeycombs.

Name	Schläfli symbol	Description
Apeirogon	$\{\infty\}$	The integer partition of $\mathbb{R}^1$
Tessellation of Triangles	$\{3,6\}$	Tiling of the plane by regular triangles
Tessellation of Hexagons	$\{6,3\}$	Tiling of the plane by regular hexagons
Cubic Honeycomb, δ_{n+1}	$\{4,3^{n-2},4\}$	Tiling of $\mathbb{R}^n$ by regular cubes, $n \geq 2$
$h\delta_5$	$\{3,3,4,3\}$	Tiling of $\mathbb{R}^4$ by crosspolytopes
Reciprocal of $h\delta_5$	$\{3,4,3,3\}$	Tiling of $\mathbb{R}^4$ by 24-cells

https://doi.org/10.4153/CJM-2005-033-6 Published online by Cambridge University Press

A key tool we will use to help us prove Theorem 3.4 will be the Coxeter groups of the honeycombs, and so it is worth noting that the symmetry groups of regular honeycombs are known to be affine Coxeter groups.

Proof It suffices to show for each class of regular honeycomb H and each choice of Petrie map σ on H, given a geometrically regular realization of H, there is a line which is stabilized by ω, the Coxeter element corresponding to the action of σ on a choice of base flag. This stable line is analogous to the stable plane of a Coxeter element of a regular convex polytope. To establish that the honeycomb is Petrial we also need to show that the action of the Coxeter element on the line is a translation along that line. To see this, note that without loss of generality we may restrict our attention to action on the base flag F. For a Petrie scheme to fail to be acoptic, $\omega^m F \cap F \neq \varnothing$ for some m and $\omega^m F \neq F$, so $(\omega^m F)_k = F_k$ for some rank k. This is the same as saying that $\omega^m \in \langle s_0, s_2, \ldots, s_{k-1}, s_{k+1}, \ldots, s_n \rangle$, a parabolic subgroup, and $\omega^m \neq e$. Any parabolic subgroup of an affine Coxeter group is a spherical Coxeter group (possibly not irreducible, and possibly with fixed point p some point other than the origin). Thus, the distance between any point x in the space and the fixed point p is fixed by the action of the parabolic subgroup. On the other hand, if ω^m acts as a translation on points on the line, then the length $||x - p||$ cannot in general be fixed (consider, for example, the point x on the line which minimizes the distance to p). This is a contradiction. Hence, to prove that the regular honeycombs are Petrial it suffices to show that for each honeycomb H and Petrie map ω, that ω acts as a translation along the stable line.

To complete the proof it is necessary to exhibit in each case a geometric realization of the honeycomb, a Petrie map on that honeycomb and to identify the line stabilized by the Petrie map. This is relatively straightforward for the honeycomb classes other than the cubic honeycomb, and so for the sake of brevity we include only the argument for the hexagonal tiling as an example and the argument for the cubic honeycombs.

The tessellation by hexagons: Consider the tiling of the plane by regular hexagons possessing a hexagon with vertices

$$\left\{(1,0), \left(\frac{1}{2}, \frac{\sqrt{3}}{2}\right), \left(-\frac{1}{2}, \frac{\sqrt{3}}{2}\right), (-1,0), \left(-\frac{1}{2}, -\frac{\sqrt{3}}{2}\right), \left(\frac{1}{2}, -\frac{\sqrt{3}}{2}\right)\right\}.$$

We will consider the generating set of reflections to be given by:

$$s_0 : \mathbf{x} \mapsto \begin{bmatrix} -1 & 0 \\ 0 & 1 \end{bmatrix} \mathbf{x} \qquad s_1 : \mathbf{x} \mapsto \begin{bmatrix} -\frac{1}{2} & \frac{\sqrt{3}}{2} \\ \frac{\sqrt{3}}{2} & \frac{1}{2} \end{bmatrix} \mathbf{x}$$

$$s_2 : \mathbf{x} \mapsto \begin{bmatrix} 1 & 0 \\ 0 & -1 \end{bmatrix} \left(\mathbf{x} - \begin{bmatrix} 0 \\ -\frac{\sqrt{3}}{2} \end{bmatrix} \right) + \begin{bmatrix} 0 \\ -\frac{\sqrt{3}}{2} \end{bmatrix}$$

and the line $l(t) = \left(0, -\frac{\sqrt{3}}{2}\right) + t\left(\frac{3}{4}, \frac{\sqrt{3}}{4}\right)$.

https://doi.org/10.4153/CJM-2005-033-6 Published online by Cambridge University Press

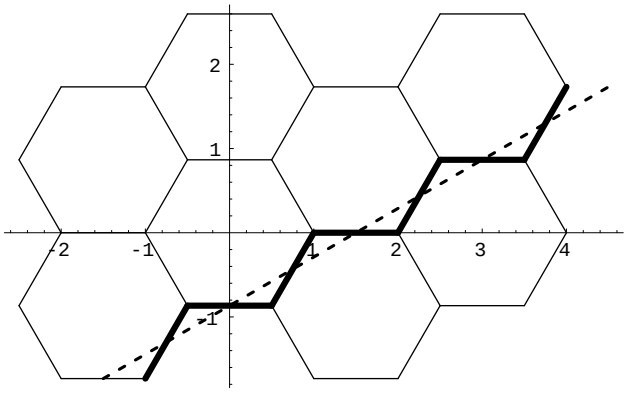

Figure 4: A portion of the tessellation of the plane by regular hexagons with a Petrie polygon indicated in bold lines and its associated stable line indicated by a dashed line.

The base flag corresponding to our choice of generating maps is given by

$$\left\{\left\{\left(-\frac{1}{2},-\frac{\sqrt{3}}{2}\right)\right\},\left\{\left(-\frac{1}{2},-\frac{\sqrt{3}}{2}\right),\left(\frac{1}{2},-\frac{\sqrt{3}}{2}\right)\right\},\right.$$
$$\left.\left\{(1,0),\left(\frac{1}{2},\frac{\sqrt{3}}{2}\right),\left(-\frac{1}{2},\frac{\sqrt{3}}{2}\right),(-1,0),\left(-\frac{1}{2},-\frac{\sqrt{3}}{2}\right),\left(\frac{1}{2},-\frac{\sqrt{3}}{2}\right)\right\}\right\};$$

the Petrie map σ is given by $\sigma = \rho_2\rho_1\rho_0$ with corresponding geometric map on the base flag $\omega = s_2s_1s_0$. Furthermore, $\omega(l(t)) = l(t+1)$. The action of ω is illustrated in Figure 4.

The cubic honeycombs, δ_{n+1}: Here we are defining the cubical tiling of $\mathbb{R}^n$ to be by cubes with edges of length 2, one of which is centered on the origin, with corners at integer points (*e.g.,* $(-1,-1,\ldots,-1)$, $(1,1,\ldots,1),\ldots$) and $n \geq 2$. The Petrie polygon and stable line discussed below are illustrated in Figure 5 for the case $n = 3$.

Our proof uses the canonical presentation of the Coxeter group of the n-cube from [19]. Specifically, the normals to the generating reflections of the group are given by $\alpha_i = \mathbf{e}_i - \mathbf{e}_{i+1}$ for $i = 1,\ldots,n-1$ and $\alpha_n = 2\mathbf{e}_n$, where $\mathbf{e}_i$ is the i-th standard basis vector. Let s_{i-1} be the matrix presentation of the reflection associated with α_i. For $i = 1,\ldots,n-1$ the matrix s_{i-1} is the permutation matrix of the permutation $(i,i+1)$. Similarly, s_{n-1} is the map taking $(x_1,x_2,\ldots,x_n) \mapsto (x_1,x_2,\ldots,x_{n-1},-x_n)$. The facet (or maximal cube) exchange map is defined to be $s_n\mathbf{x} = (\mathbf{x}-\mathbf{e}_1)-2((\mathbf{x}-\mathbf{e}_1)\cdot\mathbf{e}_1)\mathbf{e}_1+\mathbf{e}_1$; in other words,

$$s_n : \mathbf{x} \mapsto (-x_1+2, x_2, \ldots, x_n).$$

Note that s_i exchanges two flags differing only at rank i. We may define a Petrie map $\omega = s_ns_0\cdots s_{n-1}$, so $\omega\mathbf{x} = (x_n+2, x_1, x_2, \ldots, x_{n-1})$.

https://doi.org/10.4153/CJM-2005-033-6 Published online by Cambridge University Press

Now consider the line $l(t) = \frac{1}{n}(n-1, n-3, \ldots, 3-n, 1-n) + \frac{t}{n}(1, 1, \ldots, 1)$. Since the action of ω on $\mathbb{R}^n$ is faithful and discrete, and since it is straightforward to show $\omega l(t) = l(t+2)$, $l(t)$ is stabilized by ω, so δ_{n+1} is Petrial. ■

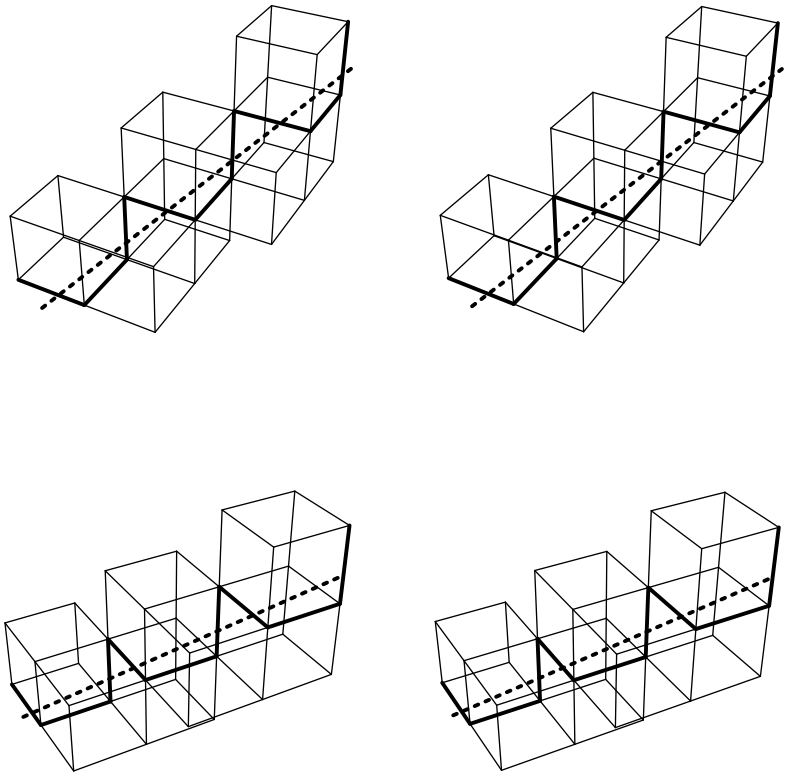

Figure 5: Two stereograms of a portion of the tessellation of 3-space by cubes, with a Petrie polygon indicated in bold lines and its associated stable line indicated by a dashed line.

3.3 The Regular Polyhedra

In 1977 [16], Grünbaum proposed a new and more comprehensive approach for defining regular polyhedra. Central to this was a consistent way of defining polygons

https://doi.org/10.4153/CJM-2005-033-6 Published online by Cambridge University Press

that took into account both non-planar polygons and non-finite polygons. These polyhedra are now known collectively as the *Grünbaum–Dress polyhedra*.

A *finite polygon* or *n-gon* $p = [V_1, V_2, \ldots, V_n]$ in Euclidean space $\mathbb{R}^d$ is a collection of vertices V_i which are distinct points in $\mathbb{R}^d$, and edges which are the line segments determined by the vertices of the polygon in consecutive pairs $\{V_i, V_{i+1}\}$, where the indices are taken modulo n. An *infinite polygon* $p = [\ldots, V_0, V_1, V_2, \ldots]$ has vertices V_i which are distinct points in $\mathbb{R}^d$ and edges that are line segements with endpoints $\{V_i, V_{i+1}\}$. The edge set is assumed to be locally finite, so that every compact set in $\mathbb{R}^d$ intersects at most a finite number of edges. A polygon p is *regular* if its symmetry group acts transitively on the flags of p.

A *polyhedron* P is any family of polygons in $\mathbb{R}^3$ which satisfy the following properties:

(1) each edge of a face is an edge of just one other face;
(2) the family of polygons is connected (in the sense of abstract polytopes);
(3) each compact set meets only finitely many faces.

Any such polyhedron satisfies the criteria for being an abstract polytope when considered as a poset. A polyhedron is *regular* if its symmetry group acts transitively on its flags.

One useful fact appears in S. Wilson's thesis [27] and is summarized by Lemma 3.5; note that πP is the polyhedron which has the same edges and vertices as P, but whose polygonal faces are the Petrie polygons of P. It will be referred to as the *Petrie dual of P*.

Lemma 3.5 *If P is a regular polyhedron, then so is πP; moreover, $\pi\pi P = P$.*

The *dual* of a Petrie scheme is the same sequence of flags with the partial order on P reversed.

Lemma 3.6 *If P is an abstract polytope, then the Petrie schemes of the dual polytope P^* are the duals of the Petrie schemes of P. Thus, if P is Petrial, so is P^*.*

Proof To prove this, observe that both $\sigma_1 = \rho_{n-1}\rho_{n-2}\cdots\rho_0$ and $\sigma_2 = \rho_0\rho_1\cdots\rho_{n-1}$ are Petrie maps of P and P^*. In other words, inverting the ranks of the elements in a Petrie scheme will yield a Petrie scheme for the dual polytope with a correspondingly inverted sequence of exchange maps in the Petrie map. ∎

Lemma 3.7 *If P is a Petrial polyhedron, then so is πP.*

Proof Recall that the Petrie polygons of πP are the polygons of P, so in particular, πP is $\{0, 1\}$-Petrial. Fix a Petrie polygon of πP (*i.e.,* a polygon p of P). P is assumed to be Petrial, so p appears at most once in any Petrie scheme of P. In particular, if $\tilde{p}$ is a face of πP, then it shares either 0 edges with p or precisely 2 consecutive edges. Suppose $\{v_1, \{v_1, v_2\}, \tilde{p}_1\}$ is a starting flag in πP, $\sigma = \rho_2\rho_1\rho_0$ is the Petrie map on πP, and p is the polygon of P whose edges are the rank 1 elements generated by this map. The next flag must be $\{v_2, \{v_2, v_3\}, \tilde{p}_2\}$, where v_3 is the unique vertex of p

https://doi.org/10.4153/CJM-2005-033-6 Published online by Cambridge University Press

sharing an edge with v_2 distinct from v_1, and $\tilde{p}_2$ is the unique Petrie polygon of P distinct from $\tilde{p}_1$ containing the edge $\{v_2, v_3\}$. No other edges of $\tilde{p}_1$ occur in p, so $\tilde{p}_1$ appears exactly once in the Petrie scheme generated using the map σ and starting flag $\{v_1, \{v_1, v_2\}, \tilde{p}_1\}$. This argument holds for any choice of starting flag, so πP is Petrial. ∎

3.4 The Eight Classes of Grünbaum–Dress Polyhedra

Table 2: The list of the geometric regular polyhedra, where a polyhedron P is listed with its dual polyhedron P^* and its Petrie dual πP.

Class	No.	Description of P	Schläfli Type	M-S	P^*	πP
1		**Platonic polyhedra**				
	1	tetrahedron	$\{3,3\}$	$\{3,3\}$	1	16
	2	octahedron	$\{3,4\}$	$\{3,4\}$	3	17
	3	cube	$\{4,3\}$	$\{4,3\}$	2	18
	4	icosahedron	$\{3,5\}$	$\{3,5\}$	5	19
	5	dodecahedron	$\{5,3\}$	$\{5,3\}$	4	23
2		**Classical planar tessellations**				
	6		$\{4,4\}$	$\{4,4\}$	6	31 with $\alpha = \frac{\pi}{2}$
	7		$\{3,6\}$	$\{3,6\}$	8	33 with $\alpha = \frac{\pi}{3}$
	8		$\{6,3\}$	$\{6,3\}$	7	32 with $\alpha = \frac{2\pi}{3}$
3		**Kepler-Poinsot polyhedra**				
	9	great dodecahedron	$\{5,\frac{5}{2}\}$	$\{5,\frac{5}{2}\}$	11	21
	10	great icosahedron	$\{3,\frac{5}{2}\}$	$\{3,\frac{5}{2}\}$	12	22
	11	small stellated dodecahedron	$\{\frac{5}{2},5\}$	$\{\frac{5}{2},5\}$	9	20
	12	great stellated dodecahedron	$\{\frac{5}{2},3\}$	$\{\frac{5}{2},3\}$	10	24
4		**Coxeter-Petrie polyhedra**				
	13		$\{4,6^{\frac{\pi}{3}}/1\}$	$\{4,6\|4\}$		40
	14		$\{6,4^{48^\circ 12'}/1\}$	$\{6,4\|4\}$		42
	15		$\{6,6^{33^\circ 33'}/1\}$	$\{6,6\|3\}$		41
5		**Finite regular polyhedra with finite skew polygons as faces**				
	16		$\{4^{\frac{\pi}{3}}/1,3\}$	$\{4,3\}_3$		1
	17		$\{6^{\frac{\pi}{3}}/1,4\}$	$\{6,4\}_3$		2

Continued on next page

https://doi.org/10.4153/CJM-2005-033-6 Published online by Cambridge University Press

Class	No.	Description of P	Schläfli Type	M-S	P^*	πP
	18		$\{6^{\frac{\pi}{2}}/1,4\}$	$\{6,3\}_4$		3
	19		$\{10^{\frac{\pi}{3}}/1,5\}$	$\{10,5\}$		4
	20		$\{6^{\frac{\pi}{5}}/1,5\}$	$\{6,5\}$		11
	21		$\{6^{\frac{3\pi}{5}}/1,\frac{5}{2}\}$	$\{6,\frac{5}{2}\}$		9
	22		$\{10^{\frac{\pi}{3}}/3,\frac{5}{2}\}$	$\{\frac{10}{3},\frac{5}{2}\}$		10
	23		$\{10^{\frac{3\pi}{5}}/1,3\}$	$\{10,3\}$		5
	24		$\{10^{\frac{\pi}{5}}/3,3\}$	$\{\frac{10}{3},3\}$		12
6		**Infinite polyhedra with finite skew polygons as faces**				
	25		$\{4^{\alpha}/1,4\}$	$\{4,4\}\#\{\}$		31
	26		$\{6^{\alpha}/1,3\}$	$\{6,3\}\#\{\}$		32
	27		$\{2.3^{\alpha}/1,6\}$	$\{3,6\}\#\{\}$		33
	28		$\{6^{\frac{\pi}{3}}/1,6\}$	$\{6,6\}_4$		29
	29		$\{4^{\frac{\pi}{3}}/1,6\}$	$\{4,6\}_6$		28
	30		$\{6^{\frac{\pi}{2}}/1,4\}$	$\{6,4\}_6$		30
7		**Regular polyhedra with zig-zag polygons as faces**				
	31		$\{\infty^{\alpha},4\}$	$\{\infty,4\}_4\#\{\}^{\dagger}$		25
	32		$\{\infty^{\alpha},3\}$	$\{\infty,3\}_6\#\{\}^{\dagger\dagger}$		26
	33		$\{\infty^{\alpha},6\}$	$\{\infty,6\}_3\#\{\}^{\ddagger}$		27
	34		$\{\infty^{\alpha(b)},4^{\alpha^*(b)}/1\},\ b\neq 0$	$\{\infty,4\}_4\#\{\infty\}$		37
	35		$\{\infty^{\gamma(b)},6^{\gamma^*(b)}/1\},\ b\neq 0$	$\{\infty,6\}_3\#\{\infty\}$		38
	36		$\{\infty^{\delta(b)},2.3^{\delta^*(b)}/1\},\ b\neq 0$	$\{\infty,3\}_6\#\{\infty\}$		39
8		**Polyhedra with helical polygons as faces**				
	37		$\{\infty^{\alpha(b),\frac{\pi}{2}},4^{\alpha^*(b)}/1\},\ b\neq 0$	$\{4,4\}\#\{\infty\}$		34
	38		$\{\infty^{\gamma(b),\frac{2\pi}{3}},6^{\gamma^*(b)}/1\},\ b\neq 0$	$\{3,6\}\#\{\infty\}$		35
	39		$\{\infty^{\delta(b),\frac{\pi}{3}},2.3^{\delta^*(b)}/1\},\ b\neq 0$	$\{6,3\}\#\{\infty\}$		36
	40		$\{\infty^{\frac{\pi}{2},\frac{2\pi}{3}},6^{\frac{\pi}{3}}/1\}$	$\{\infty,6\}_{4,4}$		13
	41		$\{\infty^{\frac{2\pi}{3},\frac{\pi}{2}},6^{33^{\circ}33'}/1\}$	$\{\infty,6\}_{6,3}$		15
	42		$\{\infty^{\frac{2\pi}{3},\frac{2\pi}{3}},4^{\frac{\pi}{3}}/1\}$	$\{\infty,4\}_{6,4}$		14
	43		$\{\infty^{\frac{2\pi}{3},\frac{\pi}{2}},3\}$	$\{\infty,3\}^{(b)}$		44
	44		$\{\infty^{\frac{2\pi}{3},\frac{2\pi}{3}},3\}$	$\{\infty,3\}^{(a)}$		43
	45		$\{\infty^{\frac{\pi}{2},\frac{2\pi}{3}},4\}$	$\{\infty,4\}_{\cdot,*3}$		45

Following [12, 13, 16], we will organize the regular polyhedra into eight classes. Alternate constructions for these polyhedra and related objects are also available in [24, §7E]. In Table 2, the polyhedra are listed by Schläfli type using the notation from [12, 13, 16]; for more details on the Schläfli notation used, see [16]. For the

†When $\alpha=\pi/2$ this is $\{\infty,4\}_4$.
††When $\alpha=2\pi/3$ this is $\{\infty,3\}_6$.
‡When $\alpha=\pi/3$ this is $\{\infty,6\}_3$.

https://doi.org/10.4153/CJM-2005-033-6 Published online by Cambridge University Press

convenience of the reader, the column labeled M-S indicates the corresponding generalizations of the Schläfli symbols used in [24, §7E]. For a specific polyhedron P, the number corresponding to its dual polyhedron P^* and its Petrie dual πP are also listed. What follows is a description of each of these classes.

Class 1: Platonic polyhedra These are the surfaces of the five well known regular convex 3-dimensional polytopes.

Class 2: Classical planar tessellations There are precisely three of these tessellations (or tilings) of the plane, one each of squares, triangles and hexagons.

Class 3: Kepler–Poinsot polyhedra These polyhedra are the finite polyhedra in which the faces are convex polygons and the vertex figures are star polygons, or vice versa. Two of them were known to Kepler; all four were independently discovered by Poinsot.

Class 4: Coxeter–Petrie polyhedra In 1937, Coxeter introduced three regular polyhedra that he and his friend J. F. Petrie had recently discovered, see [9, 11, 16]. They are the infinite regular polyhedra with convex polygons as faces and antiprismatic polygons as vertex figures. Antiprismatic polygons are the ziz-zag sequences of edges obtained from the intersections of the triangles in an antiprism. Each of the Coxeter–Petrie polyhedra is a two-dimensional subcomplex of Euclidean 3-space. Their Schläfli symbols are $\{4, 6^{\pi/3}/1\}$, $\{6, 4^{33^\circ 33'}/1\}$ and $\{6, 4^{48^\circ 12'}\}$ (also denoted in [9] as $\{4, 6|4\}$, $\{6, 6|3\}$, and $\{6, 4|4\}$ respectively).

Class 5: Finite regular polyhedra with finite skew polygons as faces There are nine polyhedra in this class, and they are the Petrie polyhedra of the Platonic or Kepler–Poinsot polyhedra. These make their first known appearance in [16], as do the remaining three classes, except one of the polyhedra in the eighth class did not appear in [16] but was instead discovered in [13].

Class 6: Infinite regular polyhedra with finite skew polygons as faces These polyhedra are related to the three regular tessellations and are obtained by deforming the faces of these tessellations into skew polygons by connecting the vertices of two copies of these tessellations in parallel planes, or by constructing finite skew polygons in the tessellation of Euclidean 3-space by cubes.

Class 7: Regular polyhedra with zigzag polygons These appear either as Petrie polyhedra of the classical planar tessellations, or as Petrie polyhedra of the polyhedra in Class 8.

Class 8: Regular polyhedra with helical faces A helical polygon requires two angles be specified to determine its geometric embedding, and so the Schläfli symbol for a helical polygon will be of the form $\{\infty^{\alpha,\beta}\}$ where α and β are the requisite angles. For more details on this notation see [16]. These polyhedra, with three exceptions, arise as the Petrie polyhedra of polyhedra in classes 4 and 7. The three remaining polyhedra are labeled as 43, 44 and 45 in Table 2. Type 43 may be built up out of one-eighth of the cubical stacks in the cubic tessellation $\{4, 3, 4\}$, staggered, in each of the three canonical directions, with one helix per stack. Type 44 is the Petrie dual of type 43. The remaining type was discovered by Dress (the reader should note that there appears to be an error in Dress' description of his map α_0), and may be thought of as being a construction similar to that of cases 43 and 44, with the helices being triangular when projected along one of the helical axes. The

helices which share that axial direction project to one-sixth of the triangles in the tiling $\{3, 6\}$.

3.4.1 The Petrial Regular Polyhedra

We will now determine which of the Grünbaum–Dress polyhedra are Petrial. We summarize our findings with the following theorem.

Table 3: Table of implications necessary for the proof of Theorem 3.8

- $1 \overset{\pi}{\Longleftrightarrow} 16$
- $2 \overset{*}{\Longleftrightarrow} 3 \overset{\pi}{\Longleftrightarrow} 18$ and $2 \overset{\pi}{\Longleftrightarrow} 17$
- $4 \overset{*}{\Longleftrightarrow} 5 \overset{\pi}{\Longleftrightarrow} 23$, $4 \overset{\pi}{\Longleftrightarrow} 19$, $4 \overset{\cong}{\Longleftrightarrow} 10 \overset{*}{\Longleftrightarrow} 12 \overset{\pi}{\Longleftrightarrow} 24$ and $10 \overset{\pi}{\Longleftrightarrow} 22$
- $6 \overset{\cong}{\Longleftrightarrow} 25 \overset{\pi}{\Longleftrightarrow} 31$
- $7 \overset{*}{\Longleftrightarrow} 8 \overset{\cong}{\Longleftrightarrow} 26 \overset{\pi}{\Longleftrightarrow} 32$ and $27 \overset{\cong}{\Longleftrightarrow} 7 \overset{\pi}{\Longleftrightarrow} 33$
- $9 \overset{*}{\Longleftrightarrow} 11 \overset{\pi}{\Longleftrightarrow} 20$ and $9 \overset{\pi}{\Longleftrightarrow} 21$
- $13 \overset{\pi}{\Longleftrightarrow} 40$
- $14 \overset{\pi}{\Longleftrightarrow} 42$
- $15 \overset{\pi}{\Longleftrightarrow} 41$
- $28 \overset{\pi}{\Longleftrightarrow} 29$
- 30
- $37 \overset{\pi}{\Longleftrightarrow} 34$
- $38 \overset{\pi}{\Longleftrightarrow} 35$
- $39 \overset{\pi}{\Longleftrightarrow} 36$
- $43 \overset{\pi}{\Longleftrightarrow} 44$
- 45

Theorem 3.8 *All of the Grünbaum–Dress polyhedra are Petrial.*

Proof A certain amount of case analysis is necessary for this argument. In Table 3 is a list of cases which, if known to be Petrial, are sufficient to complete the proof, and indications of which other cases are consequences of dualization (*, Lemma 3.6) and construction of the Petrie dual (π, Lemma 3.7) with the implication symbols marked with the map which causes the implication. Note that 25–27 are combinatorially equivalent to 6–8, and since being Petrial is essentially a combinatorial property, we have also indicated those implications which may be obtained by combinatorial equivalence with the congruence symbol ($\cong$).

Thus, establishing that 1, 2, 4, 6, 7, 9, 13, 14, 15, 28, 30, 37, 38, 39, 43 and 45 are Petrial, along with Lemmas 3.6 and 3.7, implies that all of the Grünbaum–Dress polyhedra are Petrial. The Platonic polyhedra 1, 2, and 4 are Petrial as a consequence of Theorem 3.2 (or by inspection). The planar tessellations 6 and 7 were established to be Petrial in Theorem 3.4. Thus, it remains to show that the great dodecahedron (10), the Coxeter–Petrie polyhedra (13, 14 and 15), the infinite polyhedra that have finite skew polygons as faces (28 and 30), and the polyhedra with helical polygons as faces (37, 38, 39, 43 and 45) are Petrial. The great dodecahedron will be addressed using a

https://doi.org/10.4153/CJM-2005-033-6 Published online by Cambridge University Press

(mostly) combinatorial argument, and the remaining cases all depend on geometric arguments similar to those used to provide proofs for the regular honeycombs.

3.4.2 The Great Dodecahedron

We will start by labeling the vertices as indicated in Figure 6: the pentagonal faces are given by

$$\Big\{\{1,2,7,8,4\},\{9,5,1,3,8\},\{1,4,9,10,6\},\{5,1,2,11,10\},$$
$$\{1,6,11,7,3\},\{2,3,4,5,6\},\{2,7,12,10,6\},\{12,8,3,2,11\},$$
$$\{7,8,9,10,11\},\{7,12,9,4,3\},\{12,10,5,4,8\},\{12,9,5,6,11\}\Big\}.$$

If we choose our base flag to be $\{\{1\},\ \{1,2\},\ \{1,2,7,8,4\}\}$ and apply the Petrie map $\sigma = \rho_2\rho_1\rho_0$, where ρ_i is the exchange map on rank i, we obtain the Petrie scheme

$$\Big(\big\{\{1\},\{1,2\},\{1,2,7,8,4\}\big\},\quad \big\{\{2\},\{2,7\},\{2,7,12,10,6\}\big\},$$
$$\big\{\{7\},\{7,12\},\{7,12,9,4,3\}\big\},\quad \big\{\{12\},\{12,9\},\{12,9,5,6,11\}\big\},$$
$$\big\{\{9\},\{9,5\},\{9,5,1,3,8\}\big\},\quad \big\{\{5\},\{5,1\},\{5,1,2,11,10\}\big\}\Big).$$

Inspection shows that the above scheme is acoptic. Since the great dodecahedron is a regular polyhedron, the combinatorial properties of the Petrie scheme are independent of the choice of base flag.

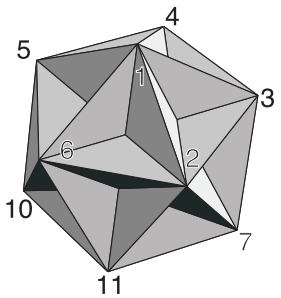

Figure 6: The great dodecahedron $\{5, \frac{5}{2}\}$. Visible vertices are labeled, and the hidden vertices are 12 (opposite 1), 8 (opposite 6), and 9 (opposite 2).

https://doi.org/10.4153/CJM-2005-033-6 Published online by Cambridge University Press

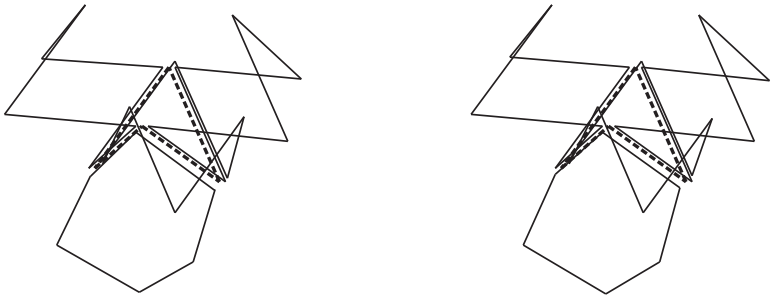

Figure 7: Stereogram of several skew hexagons of the polyhedron $\{6^{\pi/3}/1, 6\}$ intersecting a Petrie polygon in bold dashed lines. Observe that the plane which passes through the midpoints of the Petrie polygon is stabilized by the action of ω.

3.4.3 The Infinite Polyhedra 28 and 30 With Finite Skew Polygons as Faces

Type 28 is the polyhedron $\{6^{\pi/3}/1, 6\}$ whose faces are one half of the vertex figures of the Coxeter–Petrie polyhedron with square faces which met six at a vertex, $\{4, 6^{\pi/3}/1\}$. We will work with the embedding that has a polygonal face with vertices $\{(1,-1,1)\,,\,(1,1,3)\,,\,(-1,1,1)\,,\,(1,3,1)\,,\,(1,1,-1)\,,\,(3,1,1)\}$, taken in that order to form a cycle. Our base flag consists of the vertex $(1,-1,1)$, the edge

$$\{(1,-1,1)\,,(1,1,3)\}$$

and the aforementioned face. The Petrie schemes in this instance are finite, and so we are forced to inspect the actual schemes directly. The generating isometries for this base flag are quite simple, namely $s_0(x,y,z) = (2-x, 2-z, 2-y)$, $s_1(x,y,z) = (z,y,x)$ and $s_2(x,y,z) = (2-x, -2+z, 2+y)$. The Petrie scheme obtained by the application of $\omega = s_2 s_1 s_0$ to the base flag has only four elements (shown in Figure 7) and when computed is easily seen to be acoptic.

Type 30 is determined by its Schläfli type, $\{6^{\pi/2}/1, 4\}$, and may be obtained by taking one Petrie polygon in each of one half of the cubes that form the cubical tiling of $\mathbb{R}^3$, $\{4,3,4\}$. This polyhedron is self-Petrie, in the sense that the Petrie dual is of the same combinatorial type, so we need only check that the Petrie schemes are acoptic on rank 2. To do this, consider the embedding in which there is a polygon with vertices

$$\{(-1,-1,1)\,,\,(1,-1,1)\,,\,(1,-1,-1)\,,\,(1,1,-1)\,,\,(-1,1,-1)\,,\,(-1,1,1)\}$$

and a base flag consisting of the vertex $(-1,-1,1)$, the edge $\{(-1,-1,1),(1,-1,1)\}$ and the aforementioned polygon. The geometric generating maps are $s_0(x,y,z) = (-x,-z,-y)$, $s_1(x,y,z) = (y,x,z)$ and $s_2(x,y,z) = (x,-2-y,2-z)$. Without loss of generality, choose the Petrie map to be $\omega = s_2 s_1 s_0$. The orbit of ω on the given polygon is the same size as the length of the Petrie scheme, completing the proof. A Petrie polygon of the polyhedron $\{6^{\pi/2}/1, 4\}$ and its surrounding faces is illustrated in Figure 8.

https://doi.org/10.4153/CJM-2005-033-6 Published online by Cambridge University Press

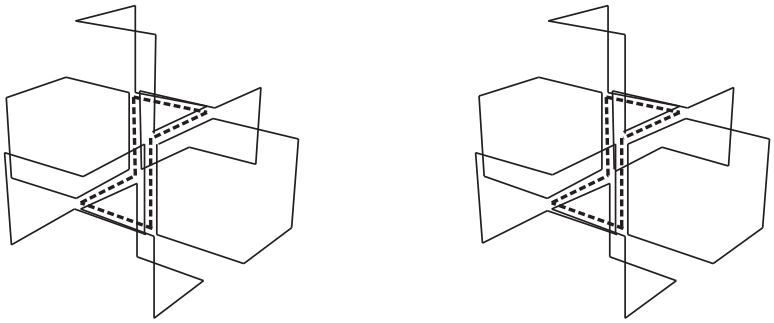

Figure 8: Stereogram of several skew hexagons of the polyhedron $\{6^{\pi/2}/1, 4\}$ intersecting a Petrie polygon in bold dashed lines. Again, the plane which passes through the midpoints of the Petrie polygon is stabilized by the action of ω.

3.4.4 The Coxeter–Petrie Polyhedra and the Polyhedra 37, 38, 39, 43 and 45 Which Have Helical Polygons as Faces

The arguments for the Coxeter–Petrie polyhedra and for polyhedra 37, 38, 39, 43 and 45 are very similar to those used for the regular honeycombs: we establish that there is a line stabilized by the action of a given Petrie map, we show the Petrie map acts as a translation along the line, and we show that no subgroup generated by a subset of the generators of the polyhedron also stabilizes the line. Note that the generating maps and either a single vertex or a choice of base flag determine the geometric realization completely, and for those types which come in a continuous family, it suffices to demonstrate that the polyhedron is Petrial for a single example, since all polyhedra in the continuous family are of the same combinatorial type. We provide only the argument for type 38, since the remaining cases differ only in computational details.

Type 38

This is the polyhedron with Schläfli symbol $\{\infty^{\gamma(b),2\pi/3}, 6^{\gamma^*(b)}/1\}$ with $b \neq 0$, where the angle functions are $\gamma(b) = \arccos\left(\frac{1-2b^2}{2+2b^2}\right)$ and $\gamma^*(b) = \arccos\left(\frac{8b^2-1}{8b^2+2}\right)$. The embedding is determined by our choice of base vertex $(0, 0, 0)$, connected by an edge to $\left(-\frac{3}{2}, \frac{\sqrt{3}}{2}, \frac{1}{\sqrt{2}}\right)$, lying in the polygon parameterized by

$$\left(\cos\left(2\pi/3t\right) - 1, \sin\left(2\pi/3t\right), t\sqrt{\tfrac{3}{2}}\right).$$

The generating maps are $s_0(x, y, z) = \left(\frac{-3-x+\sqrt{3}\,y}{2}, \frac{\sqrt{3}\,(1+x)+y}{2}, \frac{1}{\sqrt{2}} - z\right)$, $s_1(x, y, z) = (x, -y, -z)$ and $s_2(x, y, z) = \left(\frac{x-\sqrt{3}\,y}{2}, \frac{-\sqrt{3}\,x-y}{2}, z\right)$. The stabilized line is parameterized by

$$l(t) = \left(-\frac{3}{8} + \frac{3\,t}{2\sqrt{5}}, \frac{3\sqrt{3}}{8} + \sqrt{\frac{3}{20}}t, -\sqrt{\frac{2}{5}}t\right).$$

https://doi.org/10.4153/CJM-2005-033-6 Published online by Cambridge University Press

The Petrie map is $\omega = s_2 s_1 s_0$. All of the subgroups generated by subsets of $\{s_0, s_1, s_2\}$ have fixed points except for the subgroup generated by s_0 and s_1. However, $(s_1 s_0)^3$ is translation in the z direction, and $(s_0 s_1)^i$ stabilizes no point of $l(t)$ for $i = 1, 2$ and 3. ■

4 Petrie Schemes of Other Polytopes and Polyhedra

4.1 Petrie Schemes of Products of Regular Polytopes

We define the *product* of two convex polytopes P and Q as the convex hull of the set $P \times Q$ of points $\left(x_1, x_2, \ldots, x_d, y_1, y_2, \ldots, y_k\right)$ where $(x_1, x_2, \ldots, x_d) \in P$ and $\left(y_1, y_2, \ldots, y_k\right) \in Q$. The *product* of two abstract polytopes P and Q is the poset $P \times Q$ of pairs $f \times g$ where f is a non-empty face of P and g is a non-empty face of Q, and one additional element $\varnothing$. The order relation on this poset is defined as $f \times g < f' \times g'$ if $f < f'$ and $g < g'$, and $\varnothing < f \times g$ for all choices of f and g. The rank of an element $f \times g$ in $P \times Q$ is the sum of the rank of f and the rank of g, and the rank of the element $\varnothing$ is -1. The vertices, an edge, and a face of the product of a line segment and a triangle are illustrated in Figure 9. One of the real surprises of the current work is that in some cases products of regular polytopes are Petrial. In other cases, products of regular polytopes are S-Petrial for some subset S of the ranks (possessing, for example, acoptic Petrie polygons). This section aims to present what is known about these cases and to suggest directions of future exploration in this area.

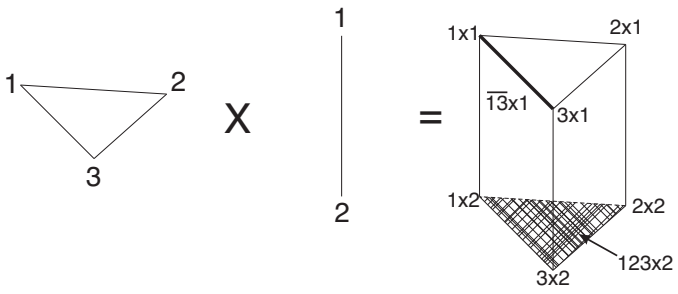

Figure 9: The product of a triangle with a line segment, with various features labeled.

4.1.1 The $4k \times 4k$ Case

We consider here the Petrie schemes in the product of two polygons P and Q which have p and q edges respectively. If P and Q are convex plane polygons then the product $P \times Q$ has a natural description in $\mathbb{R}^4$. We have the following theorem.

https://doi.org/10.4153/CJM-2005-033-6 Published online by Cambridge University Press

Theorem 4.1 *If p and q are even, with $p, q \geq 4$, then the Petrie polygons of the abstract polytope $P \times Q$ form edge disjoint circuits. If p and q are divisible by 4, then the Petrie polygons of $P \times Q$ will also form vertex disjoint circuits. Finally, if $p = q$ and is divisible by 4, then $P \times Q$ is Petrial.*

Proof Let P and Q be polytopes with p and q edges respectively. Denote the vertices of the polygons as $P = \{0, 1, 2, 3, \ldots, p-1\}$ and $Q = \{0, 1, 2, \ldots, q-1\}$; then the vertices of $P \times Q$ may be denoted by the pairs which generate them (*e.g.,* 1×1 and 1×2 which are obtained from vertex 1 of P and vertices 1 and 2 of Q). Likewise we will denote edges in $P \times Q$ by their endpoints (*e.g.,* $1 \times \overline{12}$ denotes the edge obtained by taking the product of vertex $1 \in P$ and the edge $\overline{12} \in Q$) and other faces by the products which generate them. Note that every facet of $P \times Q$ is a prism over P or Q. A maximal chain will be listed with elements in order of increasing rank separated by commas, omitting the empty set and the polytope.

In any product of polygons, every edge has precisely twelve maximal chains containing that edge, and since the polytope is isogonal and we may interchange the roles of P and Q in the argument, we may reduce the combinatorial types of the maximal chains to three. Without loss of generality, they are as follows.

$$(1) \qquad \{0 \times 0, \quad \overline{01} \times 0, \quad \overline{01} \times \overline{01}, \quad P \times \overline{01}\}$$

$$(2) \qquad \{0 \times 0, \quad \overline{01} \times 0, \quad \overline{01} \times \overline{01}, \quad \overline{01} \times Q\}$$

$$(3) \qquad \{0 \times 0, \quad \overline{01} \times 0, \quad P \times 0, \quad P \times \overline{01}\}$$

The Petrie map σ is the composition of the exchange maps ρ_i given by $\sigma = \rho_3\rho_2\rho_1\rho_0$. We need only consider the sequence of maximal chains produced by iterating the Petrie map on the chains (1), (2) and (3).

In the case of chain (1), we obtain the sequence given in Table 4. The important fact here is that the labelings mod 4 on the entry $\{4 \times 4, \overline{45} \times 4, \overline{45} \times \overline{45}, P \times \overline{45}\}$ in the table are $\{0 \times 0,\ 0 \times \overline{01},\ \overline{01} \times \overline{01},\ P \times \overline{01}\}$. Thus, the edges of $P \times Q$ may be thought of as a rectangular grid on the torus, of size $p \times q$. If p and q are divisible by 4, then there exist integers m and n such that $m = p/4$ and $n = q/4$. The grid may be divided into 4×4 blocks arranged in an $m \times n$ array. Every time the Petrie scheme leaves a 4×4 block (i, j) it will enter block $(i+1, j+1)$ (mod m and n respectively) with the same relative maximal chain in the new block as we started with in the (i, j) block. The Petrie polygon will repeat without self intersection until re-entering the maximal chain $\{0 \times 0,\ \overline{01} \times 0,\ \overline{01} \times \overline{01},\ P \times \overline{01}\}$ in the original block. The same logic applies to each of the other two cases, using the sequences given in Table 5. This is enough to complete our argument. If $p = 4k+2$ and $q = 4j$, then while the first of the three classes of schemes is vertex and edge disjoint, the latter two are merely edge disjoint. If $p = 4k+2$ and $q = 4j+2$, none of the Petrie schemes is vertex disjoint, but they are edge disjoint. If $p = 4k$ and $q = 4j$ where $k < j$ then while the schemes remain vertex and edge disjoint, the element $P \times \overline{01}$, for example, will reappear $LCM(k, j)/j$ times in the first scheme. Similar obstructions appear in the other schemes. If $p = q = 4k$ then the Petrie schemes are acoptic, for if we take

https://doi.org/10.4153/CJM-2005-033-6 Published online by Cambridge University Press

Table 4: The sequence of maximal chains for $\{0 \times 0,\ \overline{01} \times 0,\ \overline{01} \times \overline{01},\ P \times \overline{01}\}$ obtained by iterating σ.

$$\begin{aligned}
\Big(\ldots,\{0 \times 0, \quad & \overline{01} \times 0, \quad & \overline{01} \times \overline{01}, \quad & P \times \overline{01}\},\\
\{1 \times 0, \quad & 1 \times \overline{01}, \quad & \overline{12} \times \overline{01}, \quad & \overline{12} \times Q\},\\
\{1 \times 1, \quad & \overline{12} \times 1, \quad & \overline{12} \times \overline{12}, \quad & P \times \overline{12}\},\\
\{2 \times 1, \quad & 2 \times \overline{12}, \quad & \overline{23} \times \overline{12}, \quad & \overline{23} \times Q\},\\
\{2 \times 2, \quad & \overline{23} \times 2, \quad & \overline{23} \times \overline{23}, \quad & P \times \overline{23}\},\\
\{3 \times 2, \quad & 3 \times \overline{23}, \quad & \overline{34} \times \overline{23}, \quad & \overline{34} \times Q\},\\
\{3 \times 3, \quad & \overline{34} \times 3, \quad & \overline{34} \times \overline{34}, \quad & P \times \overline{34}\},\\
\{4 \times 3, \quad & 4 \times \overline{34}, \quad & \overline{45} \times \overline{34}, \quad & \overline{45} \times Q\},\\
\{4 \times 4, \quad & \overline{45} \times 4, \quad & \overline{45} \times \overline{45}, \quad & P \times \overline{45}\},\ldots\Big)
\end{aligned}$$

the final row of each of these schemes modulo 4 there is no self-intersection within a 4×4 block, and all of the blocks have independent indices.

■

4.1.2 Products of Cubes and Crosspolytopes

Polytopes that show a great deal of promise for being Petrial are the products of cubes and crosspolytopes. Working in a purely combinatorial setting, computer based analysis of the structure of the Petrie schemes (which come in several types, as in the case of polygonal products) indicate that a significant number of the products of cubes and crosspolytopes are Petrial when the dimension of the product polytope is less than or equal to six. The known results are listed in Table 6. In the table, *rank* refers to the rank of the polytope as an abstract polytope; this number corresponds to the geometric dimension of the polytope. Clearly the product of two cubes is Petrial, since such a product is also a cube, but the cases which involve crosspolytopes are more subtle, and suggest the following.

Conjecture 4.2 *The product of any two crosspolytopes is Petrial.*

Conjecture 4.3 *Every product of a combinatorial d-cube and an n-crosspolytope is Petrial.*

https://doi.org/10.4153/CJM-2005-033-6 Published online by Cambridge University Press

Table 5: The remaining sequences of maximal chains in $P \times Q$.

Scheme of flag (2)	Scheme of flag (3)
$(\ldots,$	$(\ldots,$
$\{0 \times 0, \overline{10} \times 0, \overline{01} \times \overline{01}, \overline{01} \times Q\},$	$\{0 \times 0, \overline{01} \times 0, P \times 0, P \times \overline{01}\},$
$\{1 \times 0, 1 \times \overline{01}, 1 \times Q, \overline{12} \times Q\},$	$\{1 \times 0, \overline{12} \times 0, \overline{12} \times \overline{01}, \overline{12} \times Q\},$
$\{1 \times 1, 1 \times \overline{12}, \overline{12} \times \overline{12}, P \times \overline{12}\},$	$\{2 \times 0, 2 \times \overline{01}, 2 \times Q, \overline{23} \times Q\},$
$\{1 \times 2, \overline{12} \times 2, P \times 2, P \times \overline{23}\},$	$\{2 \times 1, 2 \times \overline{12}, \overline{23} \times \overline{12}, P \times \overline{12}\},$
$\{2 \times 2, \overline{23} \times 2, \overline{23} \times \overline{23}, \overline{23} \times Q\},$	$\{2 \times 2, \overline{23} \times 2, P \times 2, P \times \overline{23}\},$
$\{3 \times 2, 3 \times \overline{23}, 3 \times Q, \overline{34} \times Q\},$	$\{3 \times 2, \overline{34} \times 2, \overline{34} \times \overline{23}, \overline{34} \times Q\},$
$\{3 \times 3, 3 \times \overline{34}, \overline{34} \times \overline{34}, P \times \overline{34}\},$	$\{4 \times 2, 4 \times \overline{23}, 4 \times Q, \overline{45} \times Q\},$
$\{3 \times 4, \overline{34} \times 4, P \times 4, P \times \overline{45}\},$	$\{4 \times 3, 4 \times \overline{34}, \overline{45} \times \overline{34}, P \times \overline{34}\},$
$\{4 \times 4, \overline{45} \times 4, \overline{45} \times \overline{45}, \overline{45} \times Q\}, \ldots)$	$\{4 \times 4, \overline{45} \times 4, P \times 4, P \times \overline{45}\}, \ldots)$

Table 6: Known cases of Petrial products of cubes and crosspolytopes.

Polytope	**Polytope**	**Rank**
line segement	octahedron	4
square	octahedron	5
3-cube	octahedron	6
octahedron	octahedron	6
line segment	4-crosspolytope	5
square	4-crosspolytope	6
d-cube	n-cube	$d + n$

4.1.3 Products of Regular Polytopes That Are Not Petrial

Computations were performed on other products of regular polytopes with limited success. Of particular interest was the fact that other products of pairs of dual polyhedra were not Petrial. The results of these computations are listed in Table 7.

There are several items of note in the current data which suggest further avenues

https://doi.org/10.4153/CJM-2005-033-6 Published online by Cambridge University Press

Table 7: Products of regular polytopes which fail to be Petrial.

Polytope	**Polytope**	**Acoptic ranks**	**Rank**
triangle	square	$\varnothing$	4
triangle	tetrahedron	$\varnothing$	5
line segment	icosahedron	$\varnothing$	4
triangle	icosahedron	$\varnothing$	5
square	icosahedron	$\{2\}$	5
pentagon	icosahedron	$\{0, 1, 2\}$	5
hexagon	icosahedron	$\varnothing$	5
heptagon	icosahedron	$\varnothing$	5
tetrahedron	icosahedron	$\{5\}$	6
dodecahedron	icosahedron	$\varnothing$	6
dodecahedron	dodecahedron	$\varnothing$	6
icosahedron	icosahedron	$\varnothing$	6
triangle	3-cube	$\varnothing$	5
pentagon	3-cube	$\varnothing$	5
hexagon	3-cube	$\{1\}$	5
heptagon	3-cube	$\varnothing$	5
octagon	3-cube	$\{0, 1\}$	5
enneagon	3-cube	$\varnothing$	5
decagon	3-cube	$\{1\}$	5
triangle	octahedron	$\varnothing$	5
pentagon	octahedron	$\varnothing$	5
hexagon	octahedron	$\{1\}$	5
heptagon	octahedron	$\varnothing$	5
octagon	octahedron	$\{0, 1\}$	5
enneagon	octahedron	$\varnothing$	5
decagon	octahedron	$\{1\}$	5

of research. In particular, more investigation of the products of $2k$-gons and $4k$-gons with cubes or crosspolytopes seems to be in order. Does the product of a $4k$-gon and a cube or crosspolytope always have acoptic Petrie polygons? Is the product of a $2k$-gon and a cube or crosspolytope always $\{1\}$-Petrial? The instances involving the icosahedron, where the schemes are acoptic at a single rank, are puzzling as well.

https://doi.org/10.4153/CJM-2005-033-6 Published online by Cambridge University Press

Another issue of great interest is which of the uniform polytopes are Petrial? This is not a trivial question, since the prisms and antiprisms are not, in general, Petrial.

4.2 Petrie Schemes of the Simplicial 4-Polytopes With 7 Or 8 Vertices

In 1967, Grünbaum and Sreedharan [17] published a complete enumeration of the simplicial 4-polytopes with 8 vertices. Also included in their list was the simplicial 3-sphere $\mathcal{M}$, which was the first known instance of a simplicial 3-sphere which did not possess a geometric realization as the boundary of a 4-polytope. A second, and final, example of this type, $\mathcal{M}'$, was discovered by Barnette [3] a few years later, and he later showed that this list of simplicial 3-spheres with 8 vertices is complete [4].

Before investigating the simplicial 4-polytopes with 8 vertices, the simplicial 4-polytopes with 7 vertices were examined. Following the notation of [17], we investigated the simplicial 3-spheres, denoted P_7^i. Analysis of the Petrie schemes was performed in *Mathematica*$^{\text{tm}}$ [26], treating these objects as abstract polytopes. There are exactly five combinatorial types to consider, and it turns out none of them are S-acoptic for any subset S of the ranks.

Analysis of the simplicial polytopes with 8 vertices was carried out in a similar manner. In the notation of [17], the simplicial polytopes with 8 vertices are given symbols of the form P_i^8 and the combinatorial types of the corresponding simple polytopes are denoted P_8^i. The only cases which were acoptic at any rank were P_{34}^8 (the 4-crosspolytope) and P_{35}^8, which is the cyclic polytope with 8 vertices in $\mathbb{R}^4$ and is not combinatorially equivalent to a regular polytope. It is acoptic only at rank 4. Neither $\mathcal{M}$ nor $\mathcal{M}'$ is Petrial on any subset of the ranks.

References

[1] J. W. Alexander, *The combinatorial theory of complexes.* Ann. of Math. **31**(1930), 292–320.
[2] A. Altshuler and L. Steinberg, *Enumeration of the quasisimplicial* 3*-spheres and* 4*-polytopes with eight vertices.* Pacific J. Math. **113**(1984), 269–288.
[3] D. Barnette, *Diagrams and Schlegel diagrams.* In: Combinatorial Structures and their Applications (Proc. Calgary Internat. Conf.), Gordon and Breach, New York, 1970, pp. 1–4.
[4] ———, *The triangulations of the* 3*-Sphere with up to* 8 *vertices.* J. Combinatorial Theory Ser. A **14**(1973), 37–53.
[5] J. Bokowski, C. Philippe, and S. Mock, *On a self dual* 3*-sphere of Peter McMullen.* Period. Math. Hungar. **39**(1999), 17–32.
[6] J. Bokowski and B. Sturmfels, *Computational Synthetic Geometry.* Lecture Notes in Mathematics 1355, Springer-Verlag, 1989.
[7] N. Bourbaki, *Lie Groups and Lie algebras.* In: Elements of Mathematics, Ch. 4–6. (A. Pressley, trans.) Springer-Verlag, Berlin, 2002.
[8] H. Bruggesser and P. Mani, *Shellable decompositions of cells and spheres.* Math. Scan. **29**(1971), 197–205.
[9] H. S. M. Coxeter *Regular skew polyhedra in three and four dimensions, and their topological analogues.* Proc. London Math. Soc. Series 2 **43**(1937), 33–62.
[10] ———, *Regular Polytopes.* Third edition. Dover Publications, New York, 1973.
[11] ———, *Twelve Geometric Essays.* Southern Illinois University Press, Carbondale, IL, 1968.
[12] A. Dress, *A combinatorial theory of Grünbaum's new regular polyhedra, Part I: Grünbaum's new regular polyhedra and their automorphism group.* Aequationes Math. **23**(1981), 252–265.
[13] ———, *A combinatorial theory of Grünbaum's new regular polyhedra, Part II: Complete enumeration.* Aequationes Math. **29**(1985), 222–243.
[14] L. Danzer and E. Schulte, *Reguläre Inzidenzkomplexe I.* Geom. Dedicata **13**(1982), 295–308.
[15] B. Grünbaum, *Convex Polytopes.* Interscience Publishers, 1967.

[16] ———, *Regular polyhedra—old and new.* Aequationes Math. **16**(1977), 1–20.
[17] B. Grünbaum and V. P. Sreedharan, *Enumeration of simplicial 4-polytopes with 8 vertices.* J. Combinatorial Theory **2**(1967), 437–465.
[18] M. I. Hartley, *All polytopes are quotients, and isomorphic polytopes are quotients by conjugate subgroups.* Discrete Comput. Geom. **21**(1999), 289–298.
[19] J. E. Humphreys, *Reflection Groups and Coxeter Groups.* Cambridge Studies in Advanced Mathematics 29. Cambridge University Press, Cambridge, 1990.
[20] P. McMullen, *On the Combinatorial Structure of Convex Polytopes.* Ph.D. dissertation, Univ. Birmingham, 1968.
[21] P. McMullen and E. Schulte, *Constructions for regular polytopes.* J. Combin. Theory Ser. A **53**(1990), 1–28 .
[22] ———, *Higher toroidal polytopes.* Adv. Math. **117**(1996), 17–51.
[23] ———, *Twisted groups and locally toroidal regular polytopes.* Trans. Amer. Math. Soc. **348**(1996), 1373–1410.
[24] ———, *Abstract Regular Polytopes.* Encyclopedia of Mathematics and its Applications 92. Cambridge University Press, Cambridge, 2002.
[25] E. Schulte, *Classification of locally toroidal regular polytopes.* In: Polytopes: Abstract, Convex and Computational (T. Bisztriczky, P. McMullen, R. Schneider and A. Ivic Weiss, eds.), NATO Adv. Sci. Inst. Ser. C Math. Phys. Sci., Kluwer, dordrecht, 1994, pp. 125–154.
[26] Wolfram Research, *Mathematica 5.0.* Wolfram Research,Champaign, IL, 2003.
[27] S. Wilson, *New Techniques for the Construction of Regular Maps.* Ph.D dissertation, University of Washington, 1976.
[28] G M. Ziegler, *Lectures on polytopes.* Graduate Texts in Mathematics 152, Springer-Verlag, New York, 1991.

Moravian College
Department of Mathematics and Computer Science
Room 219 Priscilla Payne Hurd Academic Complex
Bethlehem, Pennsylvania 18018
U.S.A.
e-mail: gordon@moravian.edu